Amido-bridged nucleic acids with small hydrophobic residues enhance hepatic tropism of antisense oligonucleotides in vivo.

Journal:	*Organic & Biomolecular Chemistry*
Manuscript ID:	OB-COM-02-2015-000242
Article Type:	Paper
Date Submitted by the Author:	04-Feb-2015

Complete List of Authors:	Yamamoto, Tsuyoshi; Osaka University, Graduate School of Pharmaceutical Sciences Yahara, Aiko; Osaka University, Graduate School of Pharmaceutical Sciences Waki, Reiko; Osaka University, Graduate School of Pharmaceutical Sciences Yasuhara, Hidenori; Osaka University, Graduate School of Pharmaceutical Sciences Wada, Fumito; Osaka University, Graduate School of Pharmaceutical Sciences Harada-Shiba, Mariko; National Cerebral and Cardiovascular Center Research Institute, Department of Molecular Innovation in Lipidology Obika, Satoshi; Osaka University, Graduate School of Pharmaceutical Sciences

Organic & Biomolecular Chemistry RSCPublishing

ARTICLE

Amido-bridged nucleic acids with small hydrophobic residues enhance hepatic tropism of antisense oligonucleotides *in vivo.*

Cite this: DOI: 10.1039/x0xx00000x

Received 00th January 2012,
Accepted 00th January 2012

DOI: 10.1039/x0xx00000x

www.rsc.org/

Tsuyoshi Yamamoto[a, b, c], Aiko Yahara[a, c], Reiko Waki[a], Hidenori Yasuhara[a, b], Fumito Wada[a, b], Mariko Harada-Shiba[b] and Satoshi Obika[a]

High scalability of a novel bicyclic nucleoside building block, amido-bridged nucleic acid (AmNA), to diversify pharmacokinetic properties of therapeutic antisense oligonucleotides is described. *N*2'-functionalization of AmNA with a variety of hydrophobic groups is straightforward. Combinations of these modules display similar antisense knockdown effects and improves cellular uptake, relative to sequence-matched conventional 2',4'-bridged nucleic acid (2',4'-BNA) *in vivo*.

Introduction

It has recently been demonstrated that naked therapeutic antisense oligonucleotides (AONs) exhibit robust systemic activity if comprising several chemically modified nucleic acid building blocks.[1] In particular, conformationally constrained nucleotides such as 2',4'-bridged nucleic acid (2',4'-BNA) [also known as locked nucleic acid (LNA)][2] in combination with phosphorothioate (PS) exhibit extraordinarily high target RNA binding and acceptable pharmacokinetics. However, only a small fraction of the administered PS–LNAs are distributed in the target tissues[3]; most of the dose is deposited subcellularly, which is undesirable.[4] Thus, overcoming the pharmacokinetic challenges of AONs is necessary to improve their potency and to address safety concerns.[5]

A number of targeted delivery strategies for antisense therapeutics have been developed, including the terminal conjugation of biofunctional molecules.[6] However, these ligands often interfere with knockdown activity, despite their advantageous effect on the pharmacokinetics of AONs. In contrast, numerous LNA analogues with unique bridging structures have been developed and refined, and apparently minor structural modification of LNA can significantly alter their biological properties.[3a, 7] However, designing and synthesizing this class of nucleotides are basically formidable. Therefore, evaluating the pharmacokinetics of AONs is formidable as well because we have only the option of evaluating them *in vivo*. On the other hand, Leumann *et al.* introduced hydrophobic side chains into the C6'-position of each tricyclo-DNA monomer through a metabolically labile ester group, then integrated these nucleotides into oligonucleotides and successfully improved cell-membrane permeability.[8] However, the effect of integration of these monomers on *in vivo* deposition remains obscure. In this context, we recently reported a promising alternative scaffold nucleoside, amido-bridged nucleic acid (AmNA),[9] which may be useful for addressing this issue (**Fig. 1**).

The furanose of AmNA is fused to five-membered γ-lactam, whose amide bond is bridging between C2' and C4' of the ribose and rigidly fixing in C3'-*endo* conformation. The AmNA-modified AONs are much less susceptible to nuclease digestion than their LNA counterparts, possibly because of the steric hindrance of the *N*2'-methyl and neighboring carbonyl groups of the amide. These modified AONs maintain LNA-like high RNA affinity and show higher *in vitro* antisense activity than their LNA counterparts. Notably, *N*2'-functionalization is usually facile (AmNA[*N*-R]), making AmNA a promising building block for AONs. Other multivalent heteroatom-containing BNAs, such as 2'-amino- LNA,[3c, 10] 2',4'-BNANC,[7f] *N*-Me-aminooxy BNA[7c] and 6'-thiolcontaining BNA,[11] are also intriguing alternatives in the same context, but *N*- or *S*-functionalized derivatives remain to be comprehensively developed.

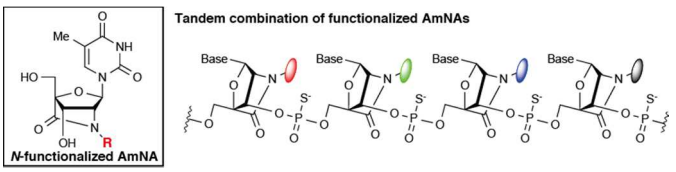

Fig. 1 Tandem arrangement strategy of *N*2'-functionalized AmNAs for improving the pharmacokinetics of antisense therapeutics.

To demonstrate the plasticity of our scaffold nucleoside for improving antisense therapeutics, we here developed a methodology to perturb the "*in vivo*" pharmacokinetics of AONs by using a variety of AmNA derivatives. Specifically, we synthesized AmNAs functionalized with a series of hydrophobic groups for potential improvement of intracellular and hepatic uptake of AONs and showed that hydrophobicity of the AmNA-AONs is readily adjustable by altering the substituents. We also

demonstrated that a better tandem combination of *N*-alkylated AmNA (AmNA[*N*-R]) modules can improve the hepatic disposition and potency of AONs *in vivo*.

Results and discussion

Phosphoramidite monomer synthesis

The phosphoramidite monomers corresponding to AmNA[*N*-H] **4a** and AmNA[*N*-Me] **4b** were obtained as previously described.[9] From known nucleoside **1**, we synthesized the five monomers AmNA[*N*-Et] **4c**, AmNA[*N*-*n*Pr] **4d**, AmNA[*N*-*i*Pr] **4e**, AmNA[*N*-Bn] **4f** and AmNA[*N*-Phen] **4g**, where abbreviated substituents indicate methyl, ethyl, *n*-propyl, *i*-propyl, benzyl and phenethyl, respectively (Scheme 1). Briefly, **1** was treated with sodium hydride, followed by addition of the corresponding alkyl halides to give *N*-substituted compounds **2a-g**. Despite steric hindrance, these coupling reactions provided high yields under optimized conditions. Hydrogenolysis of the *O*3', *O*5'-benzyl groups as well as *N*3-benzyloxymethyl groups of **2a-g** was effected using a palladium on carbon catalyst in THF followed by *O*5'-dimethoxytritylation to give *N*-substituted monomers **3a-g** in good yield over two steps (52-96%). Subsequent *O*3'-phosphitylation of **3a-g** was achieved with 2-cyanoethyl-*N,N,N',N'*-tetraisopropylphosphorodiamidite to provide desired thymine phosphoramidites **4a-g**.

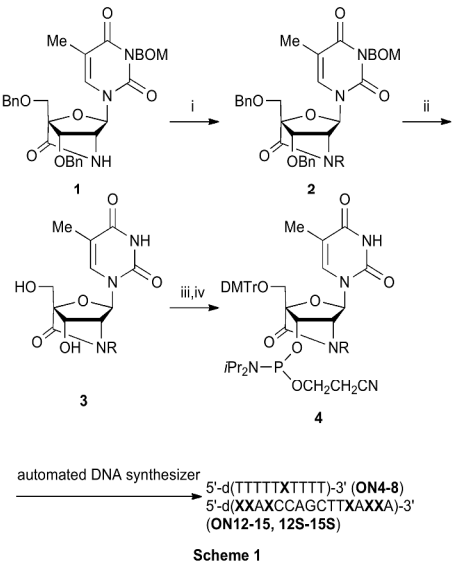

Scheme 1

Scheme 1 Reagents and conditions: i) NaH, RX, DMF, 0°C→rt, R=Et: EtBr, quant.; R=*n*Pr: *n*PrBr, 76%; R=*i*Pr: *i*PrI, quant.; R=Bn: BnBr, quant.; R=CH_2CH_2Ph: $BrCH_2CH_2Ph$, 43%; ii) 20% $Pd(OH)_2/C$, H_2, THF, rt; iii) DMTrCl, pyridine, rt, R=Et: 74% (2steps); R=*n*Pr: 96% (2steps); R=*i*Pr: 81% (2steps); R=Bn: 90% (2steps); R=CH_2CH_2Ph: 83% (2steps); iv) (*i*-$Pr_2N)_2POCH_2CH_2CN$, *N,N*-diisopropylammonium tetrazolide, MeCN/THF (3:1), rt, R=Et: 77%; R=*n*Pr: 88%; R=*i*Pr: 49%; R=Bn: 61%; R=CH_2CH_2Ph: 48%.

Oligonucleotide synthesis

Synthesis of oligonucleotides (ONs) containing AmNA[*N*-R] monomers was performed on an automated DNA synthesizer using a conventional phosphoramidite method. 5-[3,5-Bis(trifluoromethyl) phenyl]-1H-tetrazole (activator 42®) solution was used for the synthesis of all the oligonucleotides described here. *N*-Alkylated AmNAs **4a-g** were successfully coupled using an extended coupling time to 16 min. The synthesized ONs were purified by reverse-phase HPLC (RP-HPLC) and the composition and purity were analyzed by MALDI-TOF mass spectrometry and RP-HPLC, respectively (Table 1 and ESI Table S1). Purity greater than 95% was confirmed for all oligonucleotides. Note that the large-scale synthesis of phosphorothioate antisense oligonucleotides for *in vivo* usage and their purification were conducted by Gene Design Inc. (Ibaraki Japan), where they used AmNA[*N*-R] phosphoramidite monomers provided by us and the composition and purity were analyzed by MALDI-TOF mass spectrometry and RP-HPLC, respectively.

Table 1 Oligonucleotides singly modified with AmNAs.

Oligonucleotides	ID	T_m (ΔT_m / mod.) (°C)		Retention time (min)
		RNA	DNA	
5'-d(TTTTTTTTTT)-3'	**ON-1**	19	21	8.4
5'-d(TTTTTt_HTTTT)-3'	**ON-2**	26 (+7)	20 (-1)	7.1
5'-d(TTTTTt_MTTTT)-3'	**ON-3**	26 (+7)	18 (-3)	10.7
5'-d(TTTTTt_ETTTT)-3'	**ON-4**	24 (+5)	18 (-3)	13.5
5'-d(TTTTTt_nTTTT)-3'	**ON-5**	21 (+2)	18 (-3)	15.5
5'-d(TTTTTt_iTTTT)-3'	**ON-6**	22 (+3)	17 (-4)	17.0
5'-d(TTTTTt_BTTTT)-3'	**ON-7**	23 (+4)	18 (-3)	22.4
5'-d(TTTTTt_PTTTT)-3'	**ON-8**	21 (+2)	18 (-3)	25.8

t(H) = AmNA [*N*-H], t(M) = AmNA [*N*-Me], t(E) = AmNA [*N*-Et] , t(*n*) = AmNA[*N*-*n*Pr], t(*i*) = AmNA[*N*-*i*Pr], t(B) = AmNA[*N*-Bn], and t(P) = AmNA[*N*-Phen]. Conditions: eluent A: 0.1 M TEAA buffer, eluent B: A/MeCN (1/1, v/v), gradient: MeCN conc. = 8-13% (30 min), 260 nm.

Physicochemical properties of AmNA-containing oligonucleotides

We compared the relative hydrophobicity of oligonucleotides singly modified with AmNAs (**4a-g; ON-1-8**) by RP-HPLC using an octadecyl (C18) silica column under the indicated conditions. The obtained retention times are shown in Table 1. AmNA[*N*-H]-modified oligonucleotide **ON-2** was the most hydrophilic. As expected, the retention times of the derivatives varied as a function of the hydrophobicity of the oligonucleotides could be adjusted by changing the substituents and their number.

To estimate the effect of modifications (**4a-g**) on duplex stability, the thermal stability of duplexes was measured with unmodified complementary RNA and DNA strands and compared with the melting temperatures of the corresponding unmodified reference duplexes (Table 1). Single incorporation of AmNAs **4a-g** into the center of a DNA T decamer increased thermal stability for complementary RNA (ΔT_m = +2 ~ +7 ºC), but decreased stability for complementary DNA (ΔT_m = –1 ~ –4 ºC), indicating that high RNA-selective binding is maintained. These results are consistent with previous observations made using a series of BNAs whose bridges deffered in size and

composition from LNA.[7a, 12] A previous crystal structure study of DNA-LNA heteroduplex revealed that the 2'-oxygen of LNA forms hydrogen bonds with water molecules.[13] The perturbation of these hydration patterns by the 2'-substituents of AmNAs probably affected duplex stability, but all derivatives retained high affinity.

Nuclease stability

The effect of AmNA modification on nuclease resistance was determined by incorporating AmNAs into the second base from the 3'-end of oligonucleotides, followed by incubation with CAPV 40 min at 37ºC. The percentages of intact oligonucleotides was analyzed by RP-HPLC and found to be higher than with conventional AmNA[*N*-Me] (ESI Fig. S5). [7a]

In vivo activities of AmNA-modified antisense oligonucleotides

We next evaluated hydrophobic AmNA-modified AONs *in vivo*. We previously developed a potent LNA-based AON that targets apolipoprotein CIII (apoC-III) for the treatment of dyslipidemia.[14] Truncated versions of this apoC-III AON were used in these *in vivo* studies because we recently revealed these could be more potent.[3d, 15] Six LNAs were incorporated into a 16-mer PS-AON, **ON-9S**. **ON-10S** retains a seven natural-nucleotide gap moiety, sufficient for maintaining RNase H (a key enzyme for antisense mechanism)-recruiting activity.

The primary purpose of the *in vivo* study was to confirm the effectiveness of this truncated version of LNA-AON to target apoC-III mRNA, mice were dosed intravenously with **ON-10S** at a dose range of 5 to 20 mg kg^{-1}. The expression levels of apoC-III mRNA in the liver were analysed 72 hours post-injection. Dose-dependent reduction in hepatic apoC-III mRNA through a single administration of **ON-10S** was observed without significant toxicity (ESI Fig. S6, S7. The highest reduction in hepatic apoC-III mRNA (60%) was recorded at a dose of 20 mg kg^{-1}, and statistical significance with saline control was found at doses above 10 mg kg^{-1}. Thus, hydrophobic AmNAs-carrying AONs were evaluated *in vivo* at 15 mg kg^{-1}.

Table 2 Antisense oligonucleotides targeting murine apoC-III mRNA.

Oligonucleotides	ID	T_m (ΔT_m / mod.) (°C) RNA	Retention time (min)
5'-d(TTATCCAGCTTTATTA)-3'	**ON-9S**	39	5.8
5'-d($t_Lt_LAt_LCCAGCTTt_Lt_LA$)-3'	**ON-10S**	63 (+4)	5.8
5'-d($t_Mt_MAt_MCCAGCTTt_Mt_Mt_MA$)-3'	**ON-11S**	63 (+4)	5.8
5'-d($t_it_iAt_iCCAGCTTt_it_iA$)-3'	**ON-12S**	61 (+4)	10.6
5'-d($t_Bt_BAt_BCCAGCTTt_Bt_Bt_BA$)-3'	**ON-13S**	59 (+3)	21.2
5'-d($t_it_iAt_MCCAGCTTt_Mt_it_iA$)-3'	**ON-14S**	62 (+4)	11.0
5'-d($t_Bt_MAt_MCCAGCTTt_Mt_Mt_BA$)-3'	**ON-15S**	63 (+4)	13.0

t(L) = LNA-T, t(M) = AmNA[*N*-Me], t(*i*) = AmNA[*N*-*i*Pr] and t(B) =AmNA[*N*-Bn].Conditions: eluent A: 0.1 M TEAA buffer, eluent B: A/MeCN (1/1, v/v), gradient: MeCN conc. = 13-37% (30 min), 260 nm.

N-alkylated AmNAs **4b, e, f** were introduced into PS-AON **ON-9S** to obtain **ON-11S** to **-13S** as shown in Table 2. The relative hydrophobicity of the oligonucleotides was gauged from their elution time of RP-HPLC.

Each PS modification increase the retention time of the AON; consequently the content of acetonitrile in the elution buffer was modified from 8-13% to 13-37%, as described in the footnote to Table 2. The retention times for **ON-11S** to **-13S** differed significantly and predictably from the singly-incorporated phosphodiester-version oligonucleotides (**ON-3, -6, -7**; Table 1). AmNA[*N*-Bn] **4f** and AmNA[*N*-^{i}Pr] **4e** increased the hydrophobicity of the AON, whereas steric hindrance of the gap moiety in **ON-12S** and **-13S** reduced potency. Therefore, we further designed and synthesized **ON-14S** and **-15S**, which showed well-controlled retention times. The T_m values of **ON-11S** to **-15S** were measured and found to be in approximately 60ºC under the indicated buffer condition. C57Bl/6J male mice (n = 3/group) were intravenously injected with **ON-10S, -11S, -12S, -13S, -14S** or **-15S** at a dose of 2.9 μmole kg^{-1} (15 mg kg^{-1} for **ON-10S**). LNA counterpart **ON-10S** reduced apoC-III by 45%, and AmNA-AONs **ON-11S** and **ON-12S** achieved similar knockdown of 40% and 30% respectively. This is the first demonstration of AmNA-AONs exhibiting LNA congener-like high activity *in vivo* (Fig. 2, ESI Fig. S8). In contrast, AmNA[*N*-Bn] **4f**-based AON **ON-13S** showed no knockdown. The less hindered **ON-14S** and **-15S** in the gaps showed improved potency compared to **-11S, -12S**; interestingly, **ON-14S** achieved the highest knockdown of apoC-III mRNA of the AmNA-AONs tested, suggesting that a combination of functionalized AmNAs working in tandem can tailor potency of AONs.

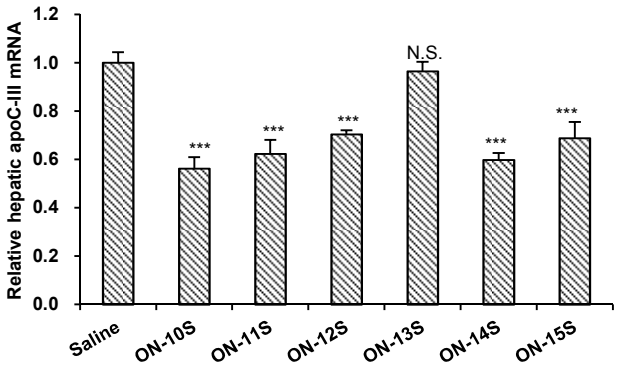

Fig. 2 Reduction of apoC-III mRNA in the livers of mice receiving a single intravenous dose of 2.868 μmole kg^{-1} of a series of AONs. Dunnett's multiple comparison test, ***P < 0.001, **P < 0.01, *P < 0.05, N.S.; not significant. Error bars represent group means + S.D. n = 3.

Hepatic tropism of hydrophobic AmNA-modified antisense oligonucleotides

To investigate whether different combinations of hydrophobic AmNAs alter the tissue deposition of AONs, we measured the intact AONs that accumulated in the liver after intravenous administration using a previously described ELISA method.[16] The hepatic distribution of the more hydrophobic **ON-12S, -13S, -14S** and **-15S** was ~1.5 times higher than that of the LNA-AON **ON-10S**, whereas **ON-10S** and **ON-11S** exhibited hepatic distribution similar to each other (Fig. 3). However,

the activity of all these AmNA-based AONs was at best comparable to the LNA counterpart **ON-10S**. It should primarily be noted that no statistical significance was found between these liver AON contents, which may contribute to this insignificant change in potency. It is also possible that the hydrophobic modification altered the suborgan distribution of AONs in liver. ApoC-III mRNA is predominantly expressed in hepatic parenchymal cells, which comprise 80% of the liver volume, whereas nonparenchymal cells such as Kupffer cells and sinusoidal endothelial cells are relatively minor components of the liver. AONs should therefore selectively target the parenchymal cells. However, it is reported that 80% of PS-AONs accumulated in the liver are distributed in nonparenchymal cells and only 20% are in the parenchymal hepetocytes.[4b] The hydrophobic AONs developed here might foster this trend. Alternatively, there are at least two uptake pathways in parenchymal cells (a productive pathway and a bulk nonproductive pathway); the hydrophobic AONs might encourage the nonproductive uptake which undermines knockdown activity of AONs.[4a]

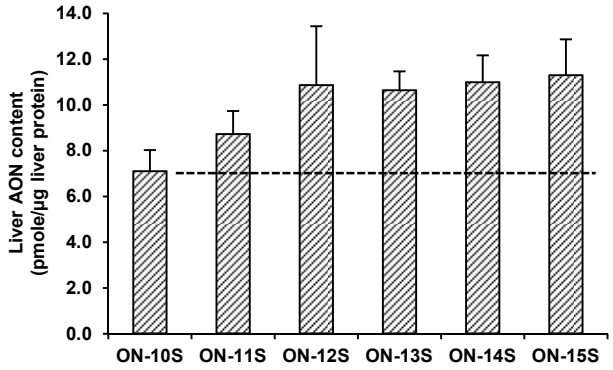

Fig. 3 ELISA-based quantification of a series of AONs distributed in murine liver after 72 hours post-injection. Error bars represent group means + S.D. $n = 3$.

Conclusions

In summary, we here showed that AmNAs are an interesting class of antisense building blocks. A series of AmNAs functionalized with a variety of hydrophobic groups were synthesized: AmNA[*N*-Et] **4c**, AmNA[*N*-*n*Pr] **4d**, AmNA[*N*-*i*Pr] **4e**, AmNA[*N*-Bn] **4f** and AmNA[*N*-Phen] **4g**. We demonstrated that a tandem arrangement of these small substituents affects the systemic activity and tissue disposition of AONs *in vivo*. This strategy will allow more finely-tuned control of the properties of AONs than conventional strategies. Using this scaffold nucleoside, we will further develop useful modules and identify the best combination of these AmNA modules to tackle the issues currently confronting antisense therapeutics.

Experimental

General

All moisture-sensitive reactions were carried out in well-dried glassware under a N_2 atmosphere. Anhydrous dichloromethane, DMF, MeCN, and pyridine were used as purchased. ^{1}H NMR spectra were recorded at 300 and 400 MHz and 500 MHz, ^{13}C NMR were recorded at 75 and 100 MHz, and the ^{31}P spectrum was recorded at 161 MHz. Chemical shift values are expressed in δ values (ppm) relative to tetramethylsilane (TMS) as internal standard and residual solvents for ^{1}H NMR, and $CHCl_3$ (δ = 77.00 ppm), methanol (δ = 49.00 ppm), and DMSO (39.50 ppm) for ^{13}C NMR, and 85% H_3PO_4 (δ = 0 ppm) for ^{31}P NMR. Fast atom bombardment mass spectra (FAB-MS) were recorded in positive ion mode. For column chromatography, silica gel PSQ 100B was used. The progress of reaction was monitored by analytical thin layer chromatography (TLC) on pre-coated aluminium sheets (Silica gel 60 F_{254}- sheet-Merck), and the products were visualized by UV light.

Synthesis of AmNA monomers and phosphoramidites.

General procedure 1 (synthesis of compound 2)

To the stirring solution of **1** (1.0 equiv.) in DMF (0.1 M) was added NaH (1.2 equiv.) at 0 °C. After stirring for 30 min, alkyl halide (1.2 equiv.) was added. The reaction temperature was gradually raised from 0 °C to room temperature and after completion of the reaction (approx. 30 min), ice-cold water was added. The solution was stirred for 15 min and the product was extracted with ethyl acetate. The organic phase was washed with brine, dried (Na_2SO_4), and concentrated. The product was purified by flash column chromatography (*n*-hexane : ethyl acetate = 3 : 1 or 2 : 1) to afford **2** as a white amorphous solid.

(2'R)-3',5'-Di-*O*-benzyl-N^3-benzyloxymethyl-2'-ethylamino-2'-*N*,4'-*C*-oxomethylenethymidine (2c: R = Et)

By following the general procedure 1, using bromoethane as an alkyl halide, **2c** was obtained in quant. as a white amorphous solid. $[\alpha]_D^{23}$ +45.9 (c 0.100, $CHCl_3$). IR (KBr): 3071, 3033, 2930, 2871, 1725, 1708, 1665, 1454, 1273 cm^{-1}. ^{1}H NMR (300 MHz, $CDCl_3$) δ : 1.22 (3H, t), 1.64 (3H, s), 3.35 (1H, dq *J* = 14 Hz, 7 Hz), 3.52 (1H, dq *J* = 14 Hz, 7 Hz), 3.95, 4.10 (2H, AB, *J* = 11.5 Hz), 4.07 (1H, s), 4.13 (1H, s), 4.52, 4.54 (2H, AB, *J* = 12 Hz), 4.59, 4.63 (2H, AB, *J* = 11.5 Hz), 4.70 (2H, s), 5.39 (1H, s), 5.45, 5.47 (2H, AB, *J* = 9.5 Hz), 7.18-7.39 (15H, m), 7.54 (1H, s). ^{13}C NMR (100 MHz, $CDCl_3$) δ :12.8, 13.7, 36.5, 62.4, 63.2, 70.1, 72.2, 72.3, 73.7, 76.7, 78.1, 85.4, 87.6, 109.8, 127.6, 127.6, 127.9, 128.1, 128.4, 133.8, 136.3, 137.4, 137.6, 150.5, 163.1, 170.1. MS (FAB): m/z 612 $[M+H]^+$. HRMS (FAB): Calcd for $C_{35}H_{38}N_3O_7$ $[M+H]^+$: 612.2710. Found: 612.2693.

(2'R)-3',5'-Di-*O*-benzyl-N^3-benzyloxymethyl-2'-propylamino-2'-*N*,4'-*C*-oxomethylenethymidine (2d: R = *n*Pr)

By following the general procedure 1, using 1-bromopropane as an alkyl halide, **2d** was obtained in 76% as a white amorphous solid. $[\alpha]_D^{23}$ +29.2 (c 1.000, $CHCl_3$). IR (KBr): 3066, 3029, 2910, 2863, 1724, 1709, 1664, 1455, 1274 cm^{-1}. ^{1}H NMR (300 MHz, $CDCl_3$) δ : 0.93 (3H, q, *J* = 7.0 Hz), 1.56-1.64 (2H, m), 1.64 (3H, s), 3.33 (2H, ddq), 3.95, 4.09 (2H, AB, *J* = 12 Hz), 4.07 (1H, s), 4.13 (1H, s), 4.53 (2H, s), 4.59, 4.65 (2H, AB, *J* = 11.0 Hz), 4.71 (2H, s), 5.40 (1H, s), 5.46 (2H, t, *J* = 9.5 Hz), 7.19-7.37 (15H, m), 7.54 (1H, s). ^{13}C NMR (100 MHz, $CDCl_3$) δ : 11.1, 12.9, 21.9, 43.4, 62.9, 63.3, 70.2, 72.3, 72.3, 72.4, 73.8, 78.2, 85.3, 87.5, 109.8, 127.6, 127.6, 127.6, 127.7, 128.0, 128.2, 128.2, 128.2, 128.4, 133.8, 136.3, 137.4, 137.4, 137.7, 150.6, 163.2, 170.5. MS (FAB): m/z 626 $[M+H]^+$. HRMS (FAB): Calcd for $C_{36}H_{40}N_3O_7$ $[M+H]^+$: 626.2866. Found: 626.2867.

(2'R)-3',5'-Di-*O*-benzyl-N^3-benzyloxymethyl-2'-isopropylamino-2'-*N*,4'-*C*-oxomethylenethymidine (2e: R = *i*Pr)

By following the general procedure 1, using 2-iodopropane as an alkyl halide, **2e** was obtained in quant. as a white amorphous solid.
$[\alpha]_D^{23}$ +57.2 (c 1.000, $CHCl_3$). IR (KBr): 3064, 3031, 2927, 2873, 1728, 1708, 1666, 1455, 1275 cm-1. ^{1}H NMR (400 MHz, $CDCl_3$) δ : 1.18 (3H, d, *J* = 7 Hz), 1.31 (3H, d, *J* = 7 Hz), 1.64 (3H, s), 3.94, 4.10 (2H, AB, *J* = 12 Hz), 4.07 (1H, s), 4.28 (1H, s), 4.36-4.47 (1H, m), 4.50, 4.54 (2H, AB, *J* = 11.5 Hz), 4.58, 4.63 (2H, AB, *J* = 11.5 Hz), 4.71 (2H, s), 5.37 (1H, s), 5.46, 5.49 (2H, AB, *J* = 9.5 Hz), 7.18-7.39 (15H, m), 7.54 (1H, s). ^{13}C NMR (100.53 MHz, $CDCl_3$) δ : 12.9, 20.6, 21.1, 42.6, 58.9, 63.2, 70.1, 72.2, 72.2, 73.7, 78.2, 86.1, 88.0, 109.6, 127.3, 127.4, 127.5, 127.6, 127.6, 127.9, 128.1, 128.2, 128.2, 128.4, 129.4, 133.8, 136.2, 137.4, 137.7, 150.5, 163.2, 169.4. MS (FAB): m/z 626 $[M+H]^+$. HRMS (FAB): Calcd for $C_{36}H_{40}N_3O_7$ $[M+H]^+$: 626.2866. Found: 626.2869.

(2'R)- 3',5'-Di-*O*-benzyl- N^3-benzyloxymethyl-2'-benzylamino-2'-*N*,4'-*C*-oxomethylenethymidine (2f: R = Bn)

By following the general procedure 1, using bromomethylbenzene as an alkyl halide, **2f** was obtained in quant. as a white amorphous solid.
$[\alpha]_D^{23}$ +17.1 (c 1.000, $CHCl_3$). IR (KBr): 3064, 3030, 2871, 1728, 1665, 1454, 1277 cm^{-1}. ^{1}H NMR (300 MHz, $CDCl_3$) δ : 1.60 (3H, s), 3.98, 4.12 (2H, AB, *J* = 12 Hz), 4.20, 4.26 (2H, AB, *J* = 11 Hz), 4.21, 4.85 (2H, AB, *J* = 15 Hz), 4.58, 4.65 (2H, AB, *J* = 11.5 Hz), 4.67 (2H, s), 5.34 (1H, s), 5.39, 5.45 (2H, AB, *J* = 9.5 Hz), 7.02-7.36 (20H, m), 7.48 (2H, s). ^{13}C NMR (100 MHz, $CDCl_3$) δ :13.0, 45.1, 61.9, 63.2, 70.3, 72.3, 72.4, 74.0, 77.8, 85.0, 87.5, 109.9, 127.5, 127.7, 127.8, 128.0, 128.1, 128.1, 128.3, 128.4, 128.6, 128.6, 128.8, 133.9, 135.8, 136.2, 137.5, 137.8, 140.0, 150.5, 151.6, 163.3, 170.5. MS (FAB): m/z 674 $[M+H]^+$. HRMS (FAB): Calcd for $C_{40}H_{40}N_3O_7$ $[M+H]^+$: 674.2866. Found: 674.2841.

(2'R)-3',5'-Di-*O*-benzyl-N^3-benzyloxymethyl-2'-phenethylamino-2'-*N*,4'-*C*-oxomethylenethymidine (2g: R = CH_2CH_2Ph)

By following the general procedure 1, using 2-bromoethylbenzene as an alkyl halide, **2g** was obtained in 43% as a white amorphous solid.
$[\alpha]_D^{24}$ +0.2 (c 0.320, $CHCl_3$). IR (KBr): 3029, 2930, 1722, 1701, 1667, 1453, 1274 cm^{-1}. ^{1}H NMR (300 MHz, $CDCl_3$) δ : 1.62 (3H, s), 2.82-3.02 (2H, m), 3.52-3.75 (2H, m), 3.94, 4.08 (2H, AB, *J* = 12 Hz), 4.02 (1H, s), 4.12 (1H, s), 4.44 (2H, s), 4.58, 4.63 (2H, AB, *J* = 11.5 Hz), 4.70 (2H, s), 5.29 (1H, s), 5.44, 5.48 (2H, AB, *J* = 9.5 Hz), 7.14-7.40 (20H, m), 7.49 (1H, s). ^{13}C NMR (100.53 MHz, $CDCl_3$) δ: 13.0, 34.7, 43.1, 63.3, 63.3, 70.3, 72.4, 72.5, 74.0, 78.3, 85.3, 87.5, 110.0, 126.7, 127.7, 127.7, 127.8, 128.1, 128.3, 128.3, 128.6, 128.6, 128.7, 133.9, 136.4, 137.5, 137.8, 137.9, 150.6, 163.3, 170.7. MS (FAB): m/z 688 $[M+H]^+$. HRMS (FAB): Calcd for $C_{41}H_{42}N_3O_7$ $[M+H]^+$: 688.3023. Found: 688.3015.

General procedure 2 (synthesis of compound 3)

To the solution of **2** (1.0 equiv.) in THF or methanol (0.1 M) was added 20 % palladium on carbon (1.0 w/w) and the reaction vessel was degassed several times with hydrogen. The reaction mixture was stirred under a hydrogen atmosphere for 1-5 h at room temperature. After completion of the reaction, the reaction solution was filtered by filter paper and washed thoroughly by hot methanol. After evaporation of solvents, the product was dissolved with methanol (0.3 M) and added 28 % ammonia solution (0.3 M) was added and the solution was stirred at room temperature. After 5 min, the product was concentrated to afford **S1** as a white solid.
To the solution of **S1** in anhydrous pyridine (0.1 M) was added DMTrCl (1.3 equiv.) and the solution was stirred at room temperature. After stirring for 1-19 h, ice-cold water was added and the product was extracted with ethyl acetate. The organic phase was washed with brine, dried (Na_2SO_4), and concentrated. The product was purified by flash column chromatography (*n*-hexane : ethyl acetate = 1 : 1 or 1 : 3) to afford **3** as a white amorphous solid.

(2'R)-5'-*O*-(4,4'-Dimethoxytrityl)-2'-ethylamino-2'-*N*,4'-*C*-oxomethylenethymidine (3c : R = Et)

By following the general procedure 2, **3c** was obtained in 45% (for 2steps) as a white amorphous solid.
$[\alpha]_D^{25}$ +12.9 (c 1.000, $CHCl_3$). IR (KBr): 3087, 2967, 2872, 1729, 1698, 1665, 1509, 1464 cm^{-1}. ^{1}H NMR (300 MHz, $CDCl_3$) δ : 1.16 (3H, t, *J* = 7 Hz), 1.62 (3H, s), 3.23-3.55 (2H, m), 3.63, 3.84 (2H, AB, *J* = 11.5 Hz), 3.74 (6H, s), 4.10 (1H, s), 4.24 (1H, s), 4.51 (1H, s), 5.39 (1H, s), 6.79-6.83 (4H, m), 7.13-7.45 (9H, m), 7.81 (1H, s), 10.33 (1H, s). ^{13}C NMR (100.53 MHz, $CDCl_3$) δ: 12.4, 13.4, 36.5, 55.1, 56.3, 64.9, 72.6, 85.3, 86.6, 88.8, 110.5, 112.9, 113.2, 127.0, 127.6, 127.8, 127.9, 129.0, 130.0, 135.1, 135.4, 144.3, 150.2, 158.4, 164.6, 170.5. MS (FAB): m/z 636 $[M+Na]^+$. HRMS (FAB): Calcd for $C_{34}H_{35}N_3O_8Na$ $[M+Na]^+$: 636.2322. Found: 636.2312.

(2'R)-5'-*O*-(4,4'-Dimethoxytrityl)-2'-propylamino-2'-*N*,4'-*C*-oxomethylenethymidine (3d: R = *n*Pr)

By following the general procedure 2, **3d** was obtained in 96% (for 2steps) as a white amorphous solid.
$[\alpha]_D^{26}$ +33.1 (c 1.000, $CHCl_3$). IR (KBr): 3384, 3021, 2838, 1704, 1699, 1509, 1254 cm^{-1}. ^{1}H NMR (300 MHz, $CDCl_3$) δ : 1.17 (3H, t, *J* = 7 Hz), 1.62 (3H, s), 3.34-3.58 (2H, m), 3.61, 3.90 (2H, AB, *J* = 12 Hz), 3.91-3.98 (2H, m), 3.88 (6H, s), 4.28 (1H, s), 4.53 (1H, d, *J* = 7 Hz), 5.50 (1H, s), 6.83-6.85 (4H, m), 7.23-7.36 (7H, m), 7.44 (2H, d, *J* = 7 Hz), 7.82 (1H, s), 9.40 (1H, s). ^{13}C NMR (75 MHz, $CDCl_3$) δ : 11.2, 12.5, 21.7, 43.6, 55.2, 56.5, 65.2, 72.8, 85.2, 86.9, 88.6, 110.7, 113.3, 113.4, 127.1, 127.9, 128.1, 130.0, 135.1, 135.3, 144.3, 150.1, 158.6, 164.3, 170.6. MS (FAB): m/z 650 $[M+Na]^+$. HRMS (FAB): Calcd for $C_{35}H_{37}N_3O_8Na$ $[M+Na]^+$: 650.2478. Found: 650.2508.

(2'R)-5'-*O*-(4,4'-Dimethoxytrityl)-2'-isopropylamino-2'-*N*,4'-*C*-oxomethylenethymidine (3e: R = *i*Pr)

By following the general procedure 2, **3e** was obtained in 78% (for 2steps) as a white amorphous solid.
$[\alpha]_D^{23}$ -3.83 (c 1.000, $CHCl_3$). IR (KBr): 3366, 3190, 2968, 2836, 1704, 1686, 1509, 1249 cm^{-1}. ^{1}H NMR (300 MHz, $CDCl_3$) δ : 1.17 (3H, d, *J* = 6.5 Hz), 1.28 (3H, d, *J* = 6.5 Hz), 1.69 (3H, s), 2.54 (1H, s), 3.59, 3.92 (2H, AB, *J* = 12 Hz), 3.77 (6H, s), 4.28 (1H, s), 4.28-4.37 (1H, m), 4.40 (1H, s), 5.37 (1H, s), 6.82-6.84 (4H, m), 7.20-7.36 (7H, m), 7.44 (2H, d, *J* = 7 Hz), 7.79 (1H, s), 9.65 (1H, s). ^{13}C NMR (100.53 MHz, $CDCl_3$): δ 12.5, 20.5, 21.1, 42.8, 55.2, 56.5, 61.5, 72.9, 86.0, 86.9, 89.2, 110.6, 113.3, 113.4, 127.1, 127.9, 128.1, 130.0, 135.2, 135.3, 144.4, 150.1,

158.6, 164.3, 169.4. MS (FAB): m/z 650 $[M+Na]^+$. HRMS (FAB): Calcd for $C_{35}H_{37}N_3O_8Na$ $[M+Na]^+$: 650.2478. Found: 650.2490.

(2'R)-5'-*O*-(4,4'-Dimethoxytrityl)-2'-benzylamino-2'-*N*,4'-*C*-oxomethylenethymidine (3f: R = Bn)

By following the general procedure 2, **3f** was obtained in 90% (for 2steps) as a white amorphous solid.
$[\alpha]_D^{25}$ +3.8 (c 1.000, $CHCl_3$). IR (KBr): 3063, 2967, 2837, 1686, 1607, 1509, 1249 cm^{-1}. ^1H NMR (300 MHz, $CDCl_3$) δ : 1.57 (3H, s), 3.67, 3.88 (2H, AB, *J* = 12 Hz), 3.74 (6H, s), 4.21 (1H, s), 4.44 (1H, s), 4.47, 4.52 (2H, AB, *J* = 15 Hz), 5.13 (1H, s), 6.79-6.83 (4H, m), 7.14-7.34 (7H, m), 7.39-7.44 (2H, d, *J* = 7 Hz), 7.74 (1H, s), 9.97 (1H, s). ^{13}C NMR (75 MHz, $CDCl_3$): δ12.5, 45.6, 55.2, 56.5, 65.1, 72.4, 84.7, 86.8, 88.7, 110.6, 113.0, 113.3, 127.1, 127.9, 128.0, 128.7, 128.8, 130.0, 135.1, 135.2, 135.7, 144.3, 150.1, 158.6, 164.4, 170.7. MS (FAB): m/z 698 $[M+Na]^+$. HRMS (FAB): Calcd for $C_{39}H_{37}N_3O_8Na$ $[M+Na]^+$: 698.2478. Found: 698.2484.

(2'R)-5'-*O*-(4,4'-Dimethoxytrityl)-2'-phenethyl amino-2'-*N*,4'-*C*-oxomethylenethymidine (3g: R = CH_2CH_2Ph)

By following the general procedure 2, **3g** was obtained in 84% (for 2steps) as a white amorphous solid.
$[\alpha]_D^{21}$ +4.6 (c 0.400, $CHCl_3$). IR (KBr): 3190, 2958, 2929, 1721, 1694, 1672, 1509, 1270 cm^{-1}.^1H NMR (300 MHz, $CDCl_3$) δ : 1.67 (3H, d, *J* = 8.5 Hz), 2.93-3.01 (2H, m), 3.56-3.66 (1H, m), 3.58, 3.87 (2H, AB, *J* = 12 Hz), 3.81 (7H, m), 4.07 (1H, s), 4.22 (1H, m), 4.34 (1H, s), 5.30 (1H, s), 6.83-7.85 (4H, m), 7.16-7.54 (14H, m), 7.72 (1H, d, *J* = 8.5 Hz), 8.61 (1H, s). ^{13}C NMR (75 MHz, $CDCl_3$) δ : 13.0, 34.7, 43.1, 63.3, 63.3, 70.3, 72.4, 72.5, 74.0, 78.3, 85.3, 87.5, 109.9, 126.7, 127.7, 127.7, 127.8, 128.1, 128.3, 128.3, 128.6, 128.6, 128.7, 133.9, 136.4, 137.5, 137.8, 137.9, 150.6, 163.3, 170.7. MS (FAB): m/z 712 $[M+Na]^+$. HRMS (FAB): Calcd for $C_{40}H_{39}N_3O_8Na$ $[M+Na]^+$: 712.2635. Found: 712.2631.

General procedure 3 (synthesis of compound 4)

To the solution of **3** (1.0 equiv.) in anhydrous MeCN-THF (3:1, 0.1 M) was added *N,N*-diisopropylammoniumtetrazolide (0.75 equiv.) and 2-cyanoethyl-*N,N,N',N'*-tetraisopropylphosphorodiamidite (1.2 equiv.). After stirring at room temperature for 9 h-19 h, ice-cold water was added and the product was extracted with ethyl acetate. The organic phase was washed with brine, dried (Na_2SO_4), and concentrated. The product was purified by flash column chromatography (0.05 eq. of triethylamine in *n*-hexane : ethyl acetate = 1 : 1) to afford **4c** (**R = Et**: 39 mg, 77%) as a white amorphous solid.

(2'R)-3'-*O*-[2-Cyanoethoxy(disopropylamino)phosphino]-5'-*O*-(4,4'-dimethoxytrityl)-2'-ethylamino-2'-*N*,4'-*C*-oxomethylenethymidine (4c: R = Et)

By following the general procedure 3, **4c** was obtained in 77% as a white amorphous solid.
M.p. 100-103 ℃ (CH_2Cl_2-hexane). ^{31}P NMR (161.83 MHz, $CDCl_3$) δ : 149.2, 150.3. MS (FAB): m/z 814 $[M+H]^+$. HRMS (FAB): Calcd for $C_{43}H_{53}N_5O_9P$ $[M+H]^+$: 814.3581. Found: 814.3588.

(2'R)-3'-*O*-[2-Cyanoethoxy(disopropylamino)phosphino]-5'-*O*-(4,4'-dimethoxytrityl)-2'-propylamino-2'-*N*,4'-*C*-oxomethylenethymidine (4d: R = *n*Pr)

By following the general procedure 3, **4d** was obtained in 88% as a white amorphous solid.
M.p. 83–86 °C (CH_2Cl_2-hexane). ^{31}P NMR (161.83 MHz, $CDCl_3$) δ : 149.8, 150.2. MS (FAB): m/z 828 $[M+H]^+$. HRMS (FAB): Calcd for $C_{44}H_{55}N_5O_9P$ $[M+H]^+$: 828.3737. Found: 828.3745.

(2'R)-3'-*O*-[2-Cyanoethoxy(disopropylamino)phosphino]-5'-*O*-(4,4'-dimethoxytrityl)-2'-isopropylamino-2'-*N*,4'-*C*-oxomethylenethymidine (4e: R = *i*Pr)

By following the general procedure 3, **4e** was obtained in 32% as a white amorphous solid.
M.p. 101–104 °C (CH_2Cl_2-hexane). ^{31}P NMR (161.83 MHz, $CDCl_3$) δ : 149.5, 151.3. MS (FAB): m/z 828 $[M+H]^+$. HRMS (FAB): Calcd for $C_{44}H_{55}N_5O_9P$ $[M+H]^+$: 828.3737. Found: 828.3729.

(2'R)-3'-*O*-[2-Cyanoethoxy(disopropylamino)phosphino]-5'-*O*-(4,4'-dimethoxytrityl)-2'-benzylamino-2'-*N*,4'-*C*-oxomethylenethymidine (4f: R = Bn)

By following the general procedure 3, **4f** was obtained in 61% as a white amorphous solid.
M.p. 99–101 °C (CH_2Cl_2-hexane). ^{31}P NMR (161.83 MHz, $CDCl_3$) δ : 150.0, 150.2. MS (FAB): m/z 876 $[M+H]^+$. HRMS (FAB): Calcd for $C_{48}H_{55}N_5O_9P$ $[M+H]^+$: 876.3737. Found: 876.3735.

(2'R)-3'-*O*-[2-Cyanoethoxy(disopropylamino)phosphino]-5'-*O*-(4,4'-dimethoxytrityl)-2'-phenethylamino-2'-*N*,4'-*C*-oxomethylenethymidine (4g: R = CH_2CH_2Ph)

By following the general procedure 3, **4g** was obtained in 48% as a white amorphous solid.
M.p. 98–101°C (CH_2Cl_2-hexane). ^{31}P NMR (161.83 MHz, $CDCl_3$) δ : 149.6, 150.8. MS (FAB): m/z 890 $[M+H]^+$. HRMS (FAB): Calcd for $C_{49}H_{57}N_5O_9P$ $[M+H]^+$: 890.3894. Found: 890.3909.

Synthesis, purification and characterization of oligonucleotides

Synthesis of 0.2 μmol scale of oligonucleotides **ON-6-44,** modified with AmNA[NMe] was performed using Oligonucleotides Synthesizer (Gene Design, ns-8) according to the standard phosphoroamidite protocol with Activator42™ (Proligo) as the activator. Dry MeCN was used to dissolve AmNA[NR]. The standard synthesis cycle was used for assembly of the reagents and synthesis of the oligonucleotides, except that the coupling time was extended to 16 minutes for AmNA[NR] monomers (The coupling time for AmNA[NMe] was 32 seconds.). The synthesis was carried out in trityl on mode and was treated with concentrated ammonium hydroxide at room temperature for 1 h to cleave the synthesized oligonucleotides from the solid support. The oligonucleotides were initially purified by Sep-pack Plus C_{18} Environmental Cartridge for The separated oligonucleotides were further purified by reverse-phase HPLC with Waters Xbridge™ Shield RP_{18} 2.5 μm (10 mm × 50 mm) columns with a linear gradient of MeCN (7-13% over 42 min for **ON-3 – 6**, **ON-11, ON-12, ON-16,** 8-15% over 42 min for **ON-7, ON-8**, 13-40% over 42 min for **ON-13**,

ON-17) in 0.1 M triethylammonium acetate (pH 7.0). The oligonucleotides were analyzed for purity by HPLC and characterized by MALDI-TOF mass spectroscopy.

UV melting experiments and melting profiles

The UV melting experiments were carried out on SHIMADZU UV-1650 spectrometer equipped with a T_m analysis accessory. Equimolecular amounts of the target RNA or DNA strand and oligonucleotide were dissolved in buffer A (10 mM phosphate buffer at pH 7.2 containing 100 mM NaCl) to give final strand concentration of 4 μM. The samples were annealed by heating the samples at 95 °C followed by slow cooling to room temperature. The melting profile was recorded at 260 nm from 0 to 70 °C (for **ON-3 – 8**), from 5 to 100 °C (for **ON-11 – 13, 16, 17**) at a scan rate of 0.5 °C /min. The T_m was calculated as the temperature of the half-dissociation of the formed duplexes, determined by the midline of the melting curve.

Enzymatic digestion study

The sample solutions were prepared by dissolving 0.75 μmol of oligonucleotides in 50 mM Tris-HCl buffer (pH 8.0) containing 10 mM $MgCl_2$. In each sample solutions, 0.175 μL *crotalus admanteus* venom phosphodiesterase (CAVP) was added and the cleavage reaction was carried out at 37 °C. A portion of each reaction mixture was removed at timed intervals and heated to 90 °C for 5 min to deactivate the nuclease. Aliquots of the timed samples were analyzed by RP-HPLC to evaluate the amount of intact oligonucleotides remaining. The percentage of intact oligonucleotide in each sample was calculated and plotted against the digestion time to obtain a degradation curve with time (**Figure S5**).

in vivo knockdown study

All animal procedures were performed in accordance with the guidelines of the Animal Care Ethics Committee of the National Cerebral and Cardiovascular Center Research Institute (Osaka, Japan). All animal studies were approved by an Institutional Review Board. C57BL/6J mice were obtained from CLEA Japan. All mice were male, and studies were initiated when animals were 8 weeks of age. Mice (n = 3/arm) were maintained on a 12 h light/12 h dark cycle and fed ad libitum. Mice were fed a normal chow (CE-2, CLEA Japan) for 2 weeks before and during treatment. Mice received single treatment of saline-formulated AONs intravenously. At the time of sacrifice after 72 hours of injection, mice were subjected to blood collection from tail veins and then anesthetized with Isoflurane (Forane, Abbott Japan) under an overnight fasting condition. Livers were harvested and snap frozen until subsequent analysis. Whole blood was collected and subjected to serum separation for subsequent analysis.

mRNA quantification

Frozen liver tissue was collected in a 2-mL tube with 1 mL of TRIzol Reagent (Life Technologies Japan) and a zirconia ball (ø 5 mm, Irie) and mechanically homogenized for 2 min at 30 oscillations per second by a TissueLyser II apparatus (Qiagen). Total RNA was isolated from the resulting suspensions according to the manufacturer's procedure. Gene expression was evaluated by a 2-step quantitative RT-PCR method. Reverse-transcription of RNA samples was performed by using a High Capacity cDNA Reverse-Transcription Kit (Applied Biosystems), and quantitative PCR was performed by TaqMan(R) Fast Universal PCR Master Mix (Applied Biosystems). The mRNA levels of target genes were normalized to the gapdh mRNA level. For murine apoC-III and gapdh mRNA quantitation, TaqMan Gene Expression Assay IDs of Mm00445670_m1 and Mm99999915_g1 were used.

ELISA method for AONs quantification in liver

Materials and reagents

The template DNA was a 25-mer DNA (5'-gaa tag cga taa taa agc tgg ata a-3'), which is complementary to **ON-9S** to **ON-15S**, with biotin at the 3'-end. The ligation probe DNA was a 9-mer DNA (5'-tcgctattc-3') with phosphate at the 5'-end and digoxigenin at the 3'-end. The template DNA and the ligation probe DNA were purchased from Japan Bio Service. Reacti-Bind NeutrAvidin-coated polystyrene strip plates were purchased from Thermo Fisher Scientific (nunc immobilizer streptavdin F96 white, 436015). The template DNA solution (100 nM) was prepared in hybridization buffer containing 60 mM Na_2HPO_4 (pH 7.4), 0.9 M NaCl, and 0.24% Tween 20. The ligation probe DNA solution (200 nM) was prepared in 1.5 units/well of T4 DNA ligase (TaKaRa) with 66 mM Tris-HCl (pH7.6), 6.6 mM $MgCl_2$, 10 mM DTT and 0.1 mM ATP.

The washing buffer used throughout the assay contained 25 mM Tris-HCl (pH 7.2), 0.15 M NaCl and 0.1% Tween 20. Anti-digoxigenin-AP antibody (Fab fragments conjugated with alkaline phosphatase) was obtained from Roche Diagnostics. A 1:2000 dilution of the antibody with 1:10 super block buffer in TBS (Pierce) was used in the assay. The alkaline phosphatase luminous substrate was prepared in 250 μM CDP-Star (Roche) with 100 mM Tris-HCl (*p*H 7.6) and 100 mM NaCl.

Assay procedures

Frozen liver tissue was collected in a 2-mL tube with 1 mL of PBS and a zirconia ball (ø 5 mm, Irie) and mechanically homogenized for 2 min at 30 oscillations per second by a TissueLyser II apparatus (Qiagen). Total protein concentrations were measured with a detergent compatible assay kit (Bio-Rad) and adjusted to 8 mg/L with PBS. The assay was performed at the concentration range of 128 pM to 1000 nM in duplicate. For the standard curve, 7 standard solutions were prepared. To AON-untreated mice liver homogenates were added **ON-10S, ON-11S, ON-12S, ON-13S, ON-14S,** and **ON-15S** solutions to prepare 7 standard samples at a range of 128 pM to 1000 nM. Next, the template DNA solution (100 μL) and standard solution (10 μL) or liver homogenates (10 μL) containing **ON-10S, ON-11S, ON-12S, ON-13S, ON-14S,** and **ON-15S** were added to Reacti-Bind Neutr Avidin-coated polystyrene strip 96-well plates and incubated at 37°C for 1 h to allow the binding of biotin to streptavidin-coated wells and hybridization. After hybridization, the plate was washed three times with 200 μL of washing buffer. Then, ligation probe DNA solution (100 μL) was added, and the plate was incubated at room temperature (15°C) for 3 h. The plate was then washed three times with the washing buffer. Subsequently, 200 μL of a 1:2000 dilution of anti-digoxigenin-AP was added, and the plate was incubated at 37°C for 1h. After washing three times with the washing buffer, CDP-Star solution was added to the plate, and finally the luminescence intensity was determined by using a Centro XS^3 luminometer (Berthold) one second after the addition of CDP-Star. The linear range of 128 pM to 1000 nM in this ELISA system was determined as $r > 0.97$.

Serum Chemistry

Serum from blood collected from the inferior vena cava upon sacrifice was subjected to serum chemistry. Assay kits (WAKO) were used to measure serum levels of aspartate aminotransferase (AST), alanine aminotransferase (ALT), which are biomarkers for hepatic toxicity.

Statistics.

Statistical comparisons were performed by Dunnett's multiple comparison tests. $*P < 0.05$, $**P < 0.001$, $***P < 0.0001$ was considered to be statistically significant in all cases. N.S. indicates no statistical significance.

Acknowledgements

This work was supported by JSPS KAKENHI Grant Number 24890102, Grants-in Aid for Scientific Research from the Japanese Ministry of Health, Labor, and Welfare (H23-seisaku tansaku-ippan-004 and H26-kanjitu-kanen-wakate-008) and a grant from the National Institute of Biomedical Innovation (09-13, 12-04). T.Y. thanks the Grant for Research on Atherosclerosis Update from the Japan Heart Foundation & Astellas/Pfizer. A. Y. thanks the Research Fellowship from the Japan Society for the Promotion of Science (JSPS) for Young Scientists.

Notes and references

[a] Graduate School of Pharmaceutical Sciences, Osaka University, 1-6 Yamadaoka, Suita, Osaka, 565-0871, Japan; Fax: +81 6 6879 8204;Tel: +81 6 6879 8200; E-mail: obika@phs.osaka-u.ac.jp

[b]Department of Molecular Innovation in Lipidology, National Cerebral and Cardiovascular Center Research Institute, 5-7-1 Fujishirodai, Suita, Osaka, 565-8565, Japan; Fax: +81 6 6872 8415;Tel: +81 6 6833 5012

[c]These authors contributed equally to this work.

1 (a) E. R. Rayburn and R. Zhang, *Drug Discov Today*, 2008, **13**, 513; (b) T. Yamamoto, M. Nakatani, K. Narukawa and S. Obika, *Future Med Chem*, 2011, **3**, 339.

2 (a) S. Obika, D. Nanbu, Y. Hari, K. Morio, Y. In, T. Ishida and T. Imanishi, *Tetrahedron Lett*, 1997, **38**, 8735; (b) S. K. Singh and J. Wengel, *Chem Commun*, 1998, 1247.

3 (a) T. Yamamoto, M. Harada-Shiba, M. Nakatani, S. Wada, H. Yasuhara, K. Narukawa, K. Sasaki, M. A. Shibata, H. Torigoe, T. Yamaoka, T. Imanishi and S. Obika, *Molecular therapy–Nucleic acids*, 2012, **1**, e22; (b) K. Fluiter, A. L. ten Asbroek, M. B. de Wissel, M. E. Jakobs, M. Wissenbach, H. Olsson, O. Olsen, H. Oerum and F. Baas, *Nucleic Acids Res*, 2003, **31**, 953; (c) K. Fluiter, M. Frieden, J. Vreijling, C. Rosenbohm, M. B. De Wissel, S. M. Christensen, T. Koch, H. Orum and F. Baas, *ChemBioChem*, 2005, **6**, 1104; (d) E. M. Straarup, N. Fisker, M. Hedtjarn, M. W. Lindholm, C. Rosenbohm, V. Aarup, H. F. Hansen, H. Orum, J. B. Hansen and T. Koch, *Nucleic Acids Res*, 2010, **38**, 7100.

4 (a) R. S. Geary, E. Wancewicz, J. Matson, M. Pearce, A. Siwkowski, E. Swayze and F. Bennett, *Biochem Pharmacol*, 2009, **78**, 284; (b) M. J. Graham, S. T. Crooke, D. K. Monteith, S. R. Cooper, K. M. Lemonidis, K. K. Stecker, M. J. Martin and R. M. Crooke, *J Pharmacol Exper Ther*, 1998, **286**, 447.

5 (a) E. E. Swayze, A. M. Siwkowski, E. V. Wancewicz, M. T. Migawa, T. K. Wyrzykiewicz, G. Hung, B. P. Monia and C. F. Bennett, *Nucleic Acids Res*, 2007, **35**, 687; (b) E. P. van Poelgeest, R. M. Swart, M. G. Betjes, M. Moerland, J. J. Weening, Y. Tessier, M. R. Hodges, A. A. Levin and J. Burggraaf, *Am J Kidney Dis*, 2013, **62**, 796.

6 (a) O. Nakagawa, X. Ming, L. Huang and R. L. Juliano, *J Am Chem Soc*, 2010, **132**, 8848; (b) T. P. Prakash, M. J. Graham, J. H. Yu, R. Carty, A. Low, A. Chappell, K. Schmidt, C. G. Zhao, M. Aghajan, H. F. Murray, S. Riney, S. L. Booten, S. F. Murray, H. Gaus, J. Crosby, W. F. Lima, S. L. Guo, B. P. Monia, E. E. Swayze and P. P. Seth, *Nucleic Acids Res*, 2014, **42**, 8796; (c) J. Winkler, *Therapeutic delivery*, 2013, **4**, 791.

7 (a) S. M. A. Rahman, S. Seki, S. Obika, H. Yoshikawa, K. Miyashita and T. Imanishi, *J Am Chem Soc*, 2008, **130**, 4886; (b) P. P. Seth, A. Siwkowski, C. R. Allerson, G. Vasquez, S. Lee, T. P. Prakash, E. V. Wancewicz, D. Witchell and E. E. Swayze, *J Med Chem*, 2009, **52**, 10; (c) T. P. Prakash, A. Siwkowski, C. R. Allerson, M. T. Migawa, S. Lee, H. J. Gaus, C. Black, P. P. Seth, E. E. Swayze and B. Bhat, *J Med Chem*, 2010, **53**, 1636; (d) P. P. Seth, C. R. Allerson, A. Berdeja, A. Siwkowski, P. S. Pallan, H. Gaus, T. P. Prakash, A. T. Watt, M. Egli and E. E. Swayze, *J Am Chem Soc*, 2010; (e) P. P. Seth, G. Vasquez, C. A. Allerson, A. Berdeja, H. Gaus, G. A. Kinberger, T. P. Prakash, M. T. Migawa, B. Bhat and E. E. Swayze, *J Org Chem*, 2010, **75**, 1569; (f) K. Miyashita, S. M. A. Rahman, S. Seki, S. Obika and T. Imanishi, *Chem Commun*, 2007, 3765.

8 J. Lietard and C. J. Leumann, *J Org Chem*, 2012, **77**, 4566.

9 A. Yahara, A. R. Shrestha, T. Yamamoto, Y. Hari, T. Osawa, M. Yamaguchi, M. Nishida, T. Kodama and S. Obika, *ChemBioChem*, 2012, **13**, 2513.

10 (a) M. W. Johannsen, L. Crispino, M. C. Wamberg, N. Kalra and J. Wengel, *Org Biomol Chem*, 2011, **9**, 243; (b) S. K. Singh, R. Kumar and J. Wengel, *J Org Chem*, 1998, **63**, 6078; (c) M. D. Sorensen, M. Petersen and J. Wengel, *Chem Commun*, 2003, 2130.

11 K. Mori, T. Kodama, T. Baba and S. Obika, *Org Biomol Chem*, 2011, **9**, 5272.

12 (a) Y. Mitsuoka, T. Kodama, R. Ohnishi, Y. Hari, T. Imanishi and S. Obika, *Nucleic Acids Res*, 2009, **37**, 1225; (b) M. Nishida, T. Baba, T. Kodama, A. Yahara, T. Imanishi and S. Obika, *Chem Commun*, 2010, **46**, 5283; (c) K. Morita, M. Takagi, C. Hasegawa, M. Kaneko, S. Tsutsumi, J. Sone, T. Ishikawa, T. Imanishi and M. Koizumi, *Bioorgan Med Chem*, 2003, **11**, 2211; (d) Y. Liu, J. Xu, M. Karimiahmadabadi, C. Zhou and J. Chattopadhyaya, *The J Org Chem*, 2010, **75**, 7112; (e) A. R. Shrestha, Y. Kotobuki, Y. Hari and S. Obika, *Chem Commun*, 2014, **50**, 575.

13 M. Egli, G. Minasov, M. Teplova, R. Kumar and J. Wengel, *Chem Commun*, 2001, 651.

14 T. Yamamoto, S. Obika, M. Nakatani, H. Yasuhara, F. Wada, E. Shibata, M. A. Shibata and M. Harada-Shiba, *Eur J Pharmacol*, 2014, **723**, 353.

15 T. Yamamoto, N. Fujii, H. Yasuhara, S. Wada, F. Wada, N. Shigesada, M. Harada-Shiba and S. Obika, *Nucleic Acid Ther*, 2014, **24**, 283.

16 (a) T. Yamamoto, M. Harada-Shiba, M. Nakatani, S. Wada, H. Yasuhara, K. Narukawa, K. Sasaki, M. A. Shibata, H. Torigoe, T. Yamaoka, T. Imanishi and S. Obika, *Molecular Therapy-Nucleic Acids*, 2012, **1**; (b) R. Z. Yu, B. Baker, A. Chappell, R. S. Geary, E. Cheung and A. A. Levin, *Anal Biochem*, 2002, **304**, 19.

